INTERDIGITATED LASER-CONTACTED SOLAR CELL ON LIQUID-PHASE CRYSTALLIZED SILICON ON GLASS

Michael Vetter[1)]*, Gema Lopez[2)], Pablo Ortega[2)], Isidro Martin[2)], Gudrun Andrä[1)], David Muñoz[3], Carlos Molpeceres[3)]
[1)] Leibniz-Institute of Photonic Technology (IPHT), Dept. Functional Interfaces, Albert-Einstein-Str. 9, 07745 Jena, Germany
[2)] Micro and Nanotechnologies Group MNT, Departament d'Enginyeria Electrònica, Universitat Politècnica de Catalunya UPC, C/ Jordi Girona 1-3, Modulo C-4, 08034 Barcelona, Spain
[3)] Centro Láser UPM, Universidad Politécnica de Madrid, Ctra. De Valencia Km 7.3, 28031 Madrid, Spain
*Corresponding author: Phone +34 616 368 575
Email: michael.vetter.privat@gmx.net

ABSTRACT: 10 μm thick liquid-phase crystallized silicon (Si) layers on 3.2 mm Borofloat 33 glass (5cm x 5cm) are fabricated by continuous wave line focus laser (808 nm). A sputtered SiO_2/SiON layer stack has been implemented as barrier layer at the glass Si interface. Solar cells with interdigitated back contact are prepared on these multi-crystalline layers by using low temperature (<400°C) Doped-by-Laser (DopLa) fabrication concept. ALD-Al_2O_3/PECVD amorphous intrinsic Si carbide (SiC_x(i)) stack for emitter passivation and a-SiC_y(i)/P-doped a-SiC_z(n)/a-SiC_x(i) stack for base passivation are deposited. With short pulse (ns) UV laser (355 nm) p-type emitter (by Al-diffusion from Al_2O_3) and point contacts with back surface field (by P-diffusion from a-SiC_z(n) layer) are fabricated on n-type mc-Si absorbers layers. Solar cell process steps are monitored by charge carrier lifetime measurements using the quasi steady-state photoconductance method. A strong dependency of charge carrier lifetime on injection level and doping density of absorbers is observed. Higher lifetimes are found for lower absorber doping concentrations. In 0.7 Ωcm LPCSG absorber highest $\tau_{eff} \approx 300$ ns corresponding to $L_{eff} > 20$ μm is found. Laser-doping and contacting using UV laser resulted in small (< 20 mV) loss of V_{oc}(1sun). Crack formation in LPCSG absorbers after laser crystallization process presents technological problems in the preparation of the interdigitated metal contact.
Keywords: multi-crystalline silicon, thin film, laser crystallization, laser doping, carrier lifetime, quasi steady-state photoconductance, IBC

1 INTRODUCTION

Liquid-phase crystallized silicon on glass (LPCSG) is a promising material to fabricate high quality silicon thin films on glass, e.g. for solar cells. A high electronic material quality is achieved by first depositing barrier layers (e.g. SiO_x, SiN_x, SiO_xN_y) and then an amorphous silicon (Si) or nano-crystalline Si layer on the glass followed by crystallization with a line focus laser or electron beam. Solar cells (≈1cm^2) made with LPCSG absorbers have shown open circuit voltage (Voc) of 649 mV (Jsc=27.3 mA/cm^2, FF=68.8%, η=12.1%) [1] demonstrating high material quality approaching highest efficient multi-crystalline wafer solar cells [2]. LPCSG could merge the advantages of crystalline silicon wafer technology with its high efficiency potential and thin film technology with low Si consumption and low cost monolithic integration for module fabrication. Therefore, LPCSG technology could be an approach to overcome the emerging limits for further cost reduction in standard wafer-based module technology. However, a suitable process technology still has to be developed.

Different fabrication concepts for the solar cell emitter, including phosphorus diffusion [3], laser processing [4], or hetero junction formation by amorphous Si layers [5] have been implemented. The fabrication of well passivated absorber contacts has become in the focus recently [6]. In this work, we implement for the first time dielectric layers namely an atomic layer deposited (ALD) aluminum oxide (Al_2O_3)/plasma-enhanced chemical vapor deposited (PECVD) amorphous intrinsic silicon carbide (SiC_x(i)) stack and a-SiC_y(i)/phosphorus (P)-doped a-SiC_z(n)/a-SiC_x(i) stack. In conjunction with short puls (ns) laser (355 nm) processing we fabricate p-type emitter (by Al-diffusion from Al_2O_3) and n-type back surface field (BSF) point contacts (by P-diffusion from a-SiC_z(n) layer) on n-type LPCSG absorbers.

2 EXPERIMENTAL

2.1 LPCSG absorber fabrication

LPCSG absorbers were processed on Borofloat 33 substrates with a sputtered SiO_2/SiON layer stack. Then, an intrinsic a-Si layer (10 μm) was deposited by e-beam evaporation. Doping of absorbers was achieved by deposition of thin (5-50 nm) highly phosphorus doped a-Si films by PECVD on the intrinsic film. Next, crystallization was performed by continuous wave line focus (13 mm long line with 0.1 mm full width at half maximum) laser irradiation at 808 nm at a scan rate of 10 mm/s and a power of 12 kW/cm^2. In this process the Si film is completely molten for some milliseconds and the doping atoms are distributed homogenously in the layer before cooling down and crystallization, forming a multi-crystalline (mc) layer. A hydrogen plasma treatment in a parallel plate reactor was performed at about 500°C for 30 minutes to passivate electronic defects in the mc-Si. The absorbers were fabricated at IPHT in Jena, Germany.

2.2 Charge carrier lifetime measurement

After hydrogen plasma treatment, a surface etch and a RCA cleaning is performed with a final HF (2%)-dip and charge carrier lifetime is measured immediately using the H-termination of the Si surface resulting from

the HF-dip as electronic surface passivation. The HF-dip provides a very good surface passivation and this first lifetime measurement gives information on the electronic quality of the absorbers at the initial stage of the solar cell fabrication process. We use injection level dependent lifetime data generated by the quasi steady-state photoconductance (PC) decay method (QSSPC) with a modified (IPHT) WCT-120 PC tool (Sinton Consulting) to characterize LPCSG absorbers [7]. This contactless method allows then a monitoring of the different solar cell process steps [8].

2.3 Solar cell fabrication

We fabricate an interdigitated back contact (IBC) solar cell scheme with 3cm x 3cm cell area on 3.2 mm Borofloat 33 (Schott) substrates going about a factor of 10 beyond the actual size of lab cells for this technology. Figure 1 presents a side view scheme of the solar cell structure (a photo of a processed LPCSG absorber is shown in Fig. 8).

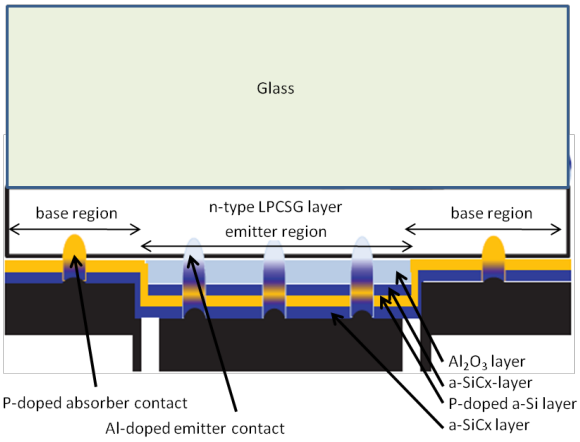

Figure 1: Side view scheme of IBC cell.

The technology is adapted from the so-called (Doped by Laser) DopLa-IBC [9] fabrication concept that has demonstrated efficiencies of 20% in wafer solar cells and is perfectly suited for the processing of solar cells on glass substrates since all process steps are performed at temperatures lower than 400°C [10, 11, 12]. In addition, the whole fabrication process includes only two lithography steps which in the future possibly also could be performed by laser-assisted processing.

3 RESULTS/DISCUSSION

Fig. 2 presents minority charge carrier lifetime curves of four LPCSG absorbers with different specific resistivity. Latter is achieved by depositing P-doped a-Si(n) layers with different thickness on the absorber before the laser crystallization process. Doping density presents strong impact on lifetime of LPCSG absorbers resulting in higher maximum lifetime for lower doping density, resp. higher resistivity. Samples with higher doping density present a stronger decay of lifetime in low injection, while samples with lower doping density present a stronger decay of lifetime in high injection. A plot of the inverse lifetime versus injection level presents a straight line in high injection. From its slope a reverse saturation current density (j_o) has been calculated (0.2 Ωcm: j_o=1.4x10^{-11}A/cm^2, 0.3 Ωcm: j_o=1.7x10^{-11}A/cm^2, 0.7 Ωcm: j_o=1.2x10^{-11}A/cm^2). The surface passivation by HF-dip of the top surface of all samples is the same. It results in a drastic reduction of surface recombination centers at the top surface. This does not create the strong dependency on injection level at high injection. Therefore, we attribute the shape of the lifetime curve at high injection to recombination properties at the glass-silicon interface. Most probably an electric field has been created at the SiON/Si interface after the laser crystallization process. A detailed analysis of the lifetime data is still under work. In any case the maximum of the lifetime of each curve gives an indication of the lower limit of the bulk lifetime and diffusion length in the absorber. The minority carrier lifetime higher than 300 ns of the n-type absorber with 0.7 Ωcm indicates a bulk diffusion length longer than 20 µm in the 10 µm thick absorber.

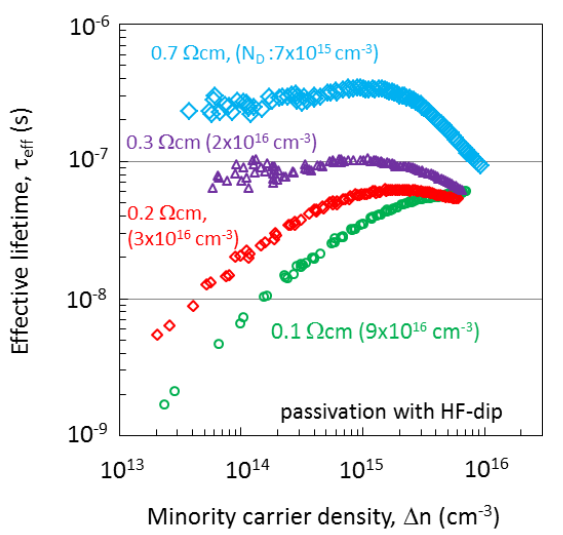

Figure 2: Lifetime curves calculated from photoconductance (PC) data of LPCSG absorbers with different specific resistivity of the mc-Si layer. A strong dependency of lifetime on injection level and doping density is observed. Data at low injection levels is limited by the sensitivity of the WCT-120 PC tool. (top surface passivation by HF-dip.

Fig. 3 shows respective Sun-V_{oc} curves calculated from the PC data of samples of Fig. 2. The slope of the Suns-Voc curve (typically between 60-120 mV/dec) gives information about recombination mechanism in the samples. One sees that the dominant recombination mechanism changes from high to low injection for all samples.

Extrapolation of Suns-V_{oc} curves to 1 sun in low and high injection parts of the curves indicates the implied V_{oc}(1sun) at standard test conditions which can be achieved under the different recombination mechanism. An example is given by the continuous black lines for the blue rhombus data of the 0.7 Ωcm sample. The high injection part indicates a V_{oc}(1sun) of 594 mV, however in low injection a recombination process reduces V_{oc}(1sun) to 552 mV.

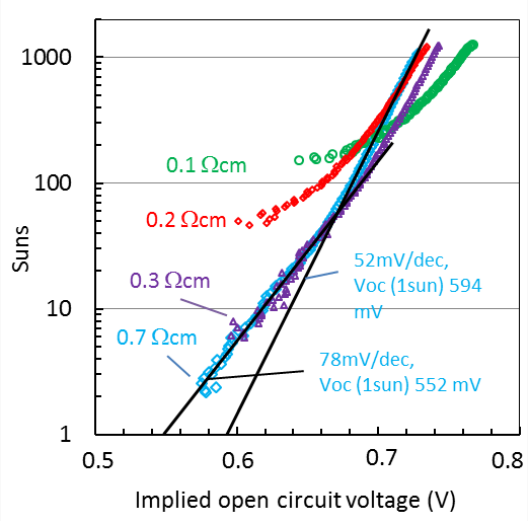

Figure 3: Sun-V_{oc} curves calculated from the PC data of samples in Fig. 2. Continuous black lines are fitting blue rhombus data of the 0.7 Ωcm sample in low resp. high injection. In this way an implied Voc (1sun) at standard test conditions is estimated for the limiting recombination mechanism in low and high injection.

Fig. 4 presents lifetime data of the 0.7 Ωcm precursor of Fig. 2 after different process steps to fabricate the interdigitated contact structure of the solar cell (see photo of a finished solar cell in Fig. 8). These processes were performed at the UPC and all details of this kind of process can be found in references [10-12].

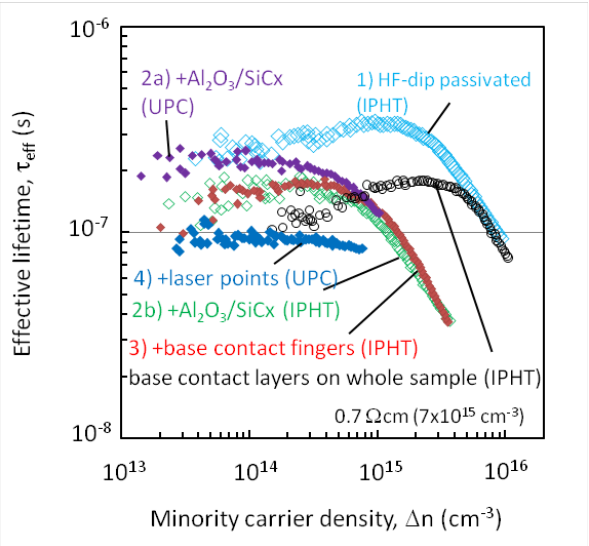

Figure 4: Lifetime data of the 0.7 Ωcm precursor of Fig. 1 after different process steps to fabricate the interdigitated contact solar cell structure.

The solar cell fabrication starts with ALD of Al_2O_3 layer and PECVD of SiC_x(i) layer which presents the basic dielectric passivation scheme of the emitter. After this process step lifetime measurement is performed at the UPC a standard WCT-120 instrument (indicated by violet rhombus and 2a) in Fig. 4) with and also at IPHT (indicated by green rhombus and 2b in Fig. 4), where the modified WCT-120 provides lifetime data at very high injection level. One sees that the data nearly coincides in the range of $\Delta n = 10^{15}$ cm^{-3} while a difference is seen at low injection levels. This might be due to slight degradation of passivation by handling and transportation. Comparing HF-dip lifetime data with the ones obtained after Al_2O_3/SiCx deposition, a clear shift of high injection lifetime to lower values can be seen, indicating that now the recombination at the top surface is dominating here. Fig. 5 presents the respective Suns-Voc curves, here we see in high injection a shift of about 20 mV to lower voltage after depositing the emitter passivation scheme. However, in low injection the change in slope is less resulting in nearly the same V_{oc}(1sun) as before.

Next, a lithography step is performed to open a window for the base passivation scheme in the emitter passivation layers. The width of the emitter fingers is about 500 µm and of the base fingers about 250 µm. Then, the SiC_y(i)/SiC_z(n)/a-SiC_x(i) layer stack for laser doping and passivation of the base contact is deposited by PECVD on the whole surface. The lifetime data after these process steps is indicated by the red rhombus and 3) and present the passivation quality of both passivation schemes side by side on the same surface. One sees that the lifetime is maintained after this process steps. To get an insight into the passivation properties of the back contact passivation scheme Fig. 4 and Fig. 5 present also a sample with a similar resistivity where the whole surface is passivated with the base passivation layer stack (shown by black circles). We see that here that in high injection the carrier lifetime decreases in the same way as with HF-dip passivation, indicating that here also the SiON/Si interface is dominating recombination, but the maximum lifetime and lifetime in low injection is lower. The SiC_y(i)/SiC_z(n)/a-SiC_x(i) back contact scheme is based on a reduction of the surface state density by the Si-rich SiC_y(i) layer and the creation of an accumulation layer by the P-doped SiC_z(n)layer (n/n+ hetero junction BSF).

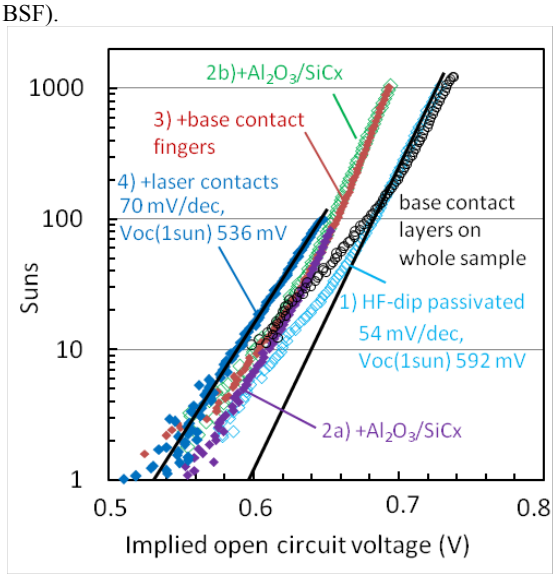

Figure 5: Respective Suns-Voc data which will be discussed in the paper (continuous black lines are fitted to the data of step 3 (red rhombus).

The next step is the fabrication of laser point contacts which has been performed by an UV laser at 355 nm. A typical laser spot is shown in Fig. 6 where the inner 9.5 µm radius presents the electrical contact area, the 14 µm

radius is limit of a "dead area" and the 19.4 μm radius is the limit of an "ablation area" where part of passivation stack is partially removed. The arrangement of laser point contacts in the base (dark) and emitter region (bright) is shown in Fig. 7. Details on the UV-laser process parameters will be published elsewhere.

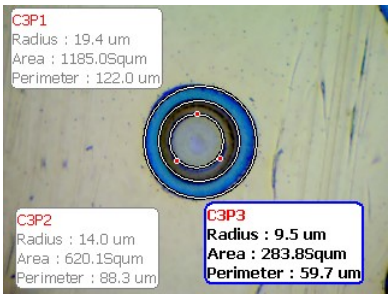

Figure 6: Typical laser spot produced with 355 nm UV laser.

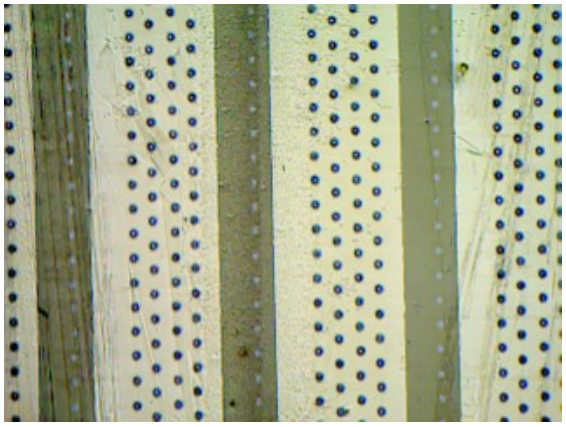

Figure 7: Arrangement of laser point contacts in the base (dark) and emitter region (bright).

The lifetime is measured after the laser process again and data is shown in Fig. 4 and 5 by the dark blue rhombus (step 4). One sees that lifetime in low injection is only reduced by a factor of two and the extrapolated V_{oc}(1sun) is 536 mV not very far from the value extrapolated at low injection of the initial measurement with HF-dip passivated surface (552 mV see Fig. 1). The emitter grid passivation consist finally in a $Al_2O_3/SiC_x(i)//SiC_y(i)/SiC_z(n)/a\text{-}SiC_x(i)$ layer stack with Al-diffused p-type emitter point contacts produced by the laser process. The absorber contact passivation scheme consists in a $SiC_y(i)/SiC_z(n)/a\text{-}SiC_x(i)$ layer stack where the laser forms point contacts with a n/n^+ BSF. Finally, electrical contacts are made by evaporation of Al on the whole top surface of the LPCSG absorber. By lithography and an etch step the emitter and base contacts are separated.

Crack formation in LPCSG absorbers after laser crystallization process presents technological problems in the preparation of the interdigitated metal contact structure. Optimization of the laser crystallization process to prevent glass bending and crack formation is necessary. Nevertheless, partial solar cells present well-rectifying diodes.

4 CONCLUSION

Quasi steady-state photoconductance method is a very helpful method to determine electronic quality of thin (about 10-20 μm) LPCSG absorbers and to monitor solar cell processing. However, sensitivity of WCT-120 photoconductance instrument limits acquisition of data in low injection. Nevertheless, lifetime and Suns-Voc curves give useful information about absorber quality and impact of process steps on recombination. In 0.7 Ωcm LPCSG absorber the $\tau_{eff} \approx 300$ ns corresponds to bulk diffusion length $L_{eff} > 20$ μm larger than the absorber thickness. Extrapolation of Sun-Voc curves in high injection indicates a limit of V_{oc}(1Sun) ≈ 600 mV representing bulk quality, however recombination in low injection reduces V_{oc}(1Sun) to about 550 mV. The similarity of Sun-V_{oc} curve and lifetime curve in high injection of H-passivated LPCSG absorber and absorber with back passivation scheme which is based on accumulation of the Si surface suggests that also at the glass/Si interface an accumulation layer is present. Simulation of charge carrier lifetime could help to better understand the different recombination mechanism and to improve surface passivation. Laser-doping and contacting applying UV laser resulted in small (<20 mV) loss of V_{oc}(1sun). Therefore, UV laser doping presents a very promising method for the fabrication of sophisticated and miniaturized contact structures.

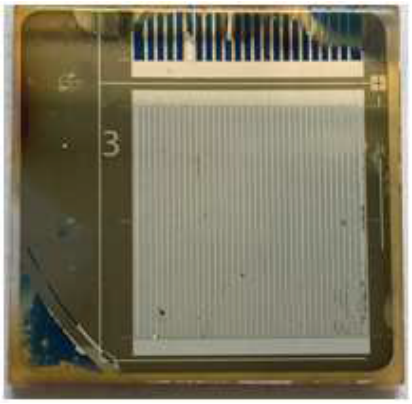

Figure 8: 5cm x 5cm solar cell with 3cm x 3cm interdigitated contact structure and metallization.

5 ACKNOWLEDGEMENT

This project has received funding from the European Union's Horizon 2020 research and innovation programme under the Marie Sklodowska-Curie grant agreement No. 657115 (cSiOnGlass, M.V.). This work has been supported by MINECO through project TEC2014-59736-R and has been funded by ENE2016-78933-C4-1-R and ENE2013-48629-C4-3-R. The authors would like also to thank the Thüringer Aufbaubank (TAB) and the European Commission (ESF) for funding the project Bi-PV (FKZ 2015 FGR 0078).

References

[1] T. Frijnts,S. Kühnapfel, S. Ring, O. Gabriel, S. Calnan, J. Haschke, B. Stannowski, B. Rech, R.Schlatmann, Sol. Energy Mater. Sol. Cells 143, (2015) 457.

[2] M. A. Green, K. Emery, Y. Hishikawa, W. Warta, E. D. Dunlop, Progr. Photovol. Res. Appl. 24 (2016) 905.

[3] J. Dore, D. Ong, S. Varlamov, R. Egan, M.A. Green, IEEE J. Photovolt.4 (1) 33 (2014).
[4] A. Gawlik, I. Höger, J. Bergmann, J. Plentz, T. Schmidt, F. Falk, and G. Andrä, Phys. Status Solidi RRL 9 (7) (2015) 397.
[5] J. Haschke, D. Amkreutz, L. Korte, F. Ruske, B. Rech B, Sol. Energy Mater. Solar Cells 128 (2014)190.
[6] P. Sonntag, J. Haschke, S. Kühnapfel, T. Frijnts, D. Amkreutz, B. Rech, Progr. Photovolt. Res. Appl. 24 (2016) 716.
[7] M. Vetter, A. Gawlik, J. Plentz, G. Andrä, Energy Procedia 92 (2016) 248.
[8] M. Vetter, A. Gawlik, J. Plentz, G. Andrä, Proc. 32nd Europ. Photovolt. Solar Energy Conf. Exh., Munich, Gernany, 2016 (WIP Munich, 2016) pp. 1100.
[9] I. Martin, M. Colina, A. Coll, G. Lopez, P. Ortega, A. Orpella, R. Alcubilla, Energy Procedia 55 (2014) 255.
[10] G. Lopez, P. Ortega, I. Martin, C. Voz, A. Orpella, R. Alcubilla, Energy Procedia 92 (2016) 652.
[11] G. Lopez Rodríguez, Interdigitated Back-contacted (IBC) c-Si solar cells based on laser processed dielectric layers, PhD Thesis, Universitat Politècnica de Catalunya, Barcelona (2016).
[12] P. Ortega, G. López, D. Muñoz, I. Martín, C. Voz, C. Molpeceres, R. Alcubilla. Sol. Energy Mater. Sol. Cells 169 (2017) 107.